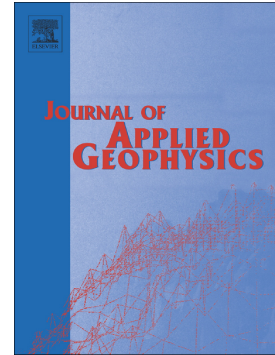


Accepted Manuscript

New method for denoising borehole transient electromagnetic data with discrete wavelet transform

Xueping Dai, Li Zhen Cheng, Jean-Claude Mareschal, Daniel Lemire, Chong Liu



PII: S0926-9851(18)30879-6
DOI: <https://doi.org/10.1016/j.jappgeo.2019.05.009>
Reference: APPGEO 3774
To appear in: *Journal of Applied Geophysics*
Received date: 31 October 2018
Revised date: 25 April 2019
Accepted date: 2 May 2019

Please cite this article as: X. Dai, L.Z. Cheng, J.-C. Mareschal, et al., New method for denoising borehole transient electromagnetic data with discrete wavelet transform, *Journal of Applied Geophysics*, <https://doi.org/10.1016/j.jappgeo.2019.05.009>

This is a PDF file of an unedited manuscript that has been accepted for publication. As a service to our customers we are providing this early version of the manuscript. The manuscript will undergo copyediting, typesetting, and review of the resulting proof before it is published in its final form. Please note that during the production process errors may be discovered which could affect the content, and all legal disclaimers that apply to the journal pertain.

NEW METHOD FOR DENOISING BOREHOLE TRANSIENT
ELECTROMAGNETIC DATA WITH DISCRETE WAVELET TRANSFORM

Xueping Dai^{1,*} xueping.dai@uqat.ca, Li Zhen Cheng¹ Li_Zhen.Cheng@uqat.ca, Jean-
Claude Mareschal² mareschal.jean-claude@uqam.ca, Daniel Lemire³
lemire@gmail.com, Chong Liu¹ chong.liu@uqat.ca

¹Université du Québec en Abitibi-Témiscamingue (UQAT), 445 Boulevard de
l'Université, Rouyn-Noranda, QC, CA, J9X 5E4

²Université du Québec à Montréal (UQAM), 405 Rue Sainte-Catherine Est, Montréal,
QC, CA, H2L 2C4

³TÉLUQ University, 455 Rue du Parvis, Québec, QC, CA, G1K 9H6

*Corresponding author.

Abstract

Discrete wavelet transform (DWT) has been widely used as a useful tool in denoising geophysical data for its outstanding feature of detecting singularities and transients. In this paper, we develop a new strategy of denoising borehole transient electromagnetic (BHTEM) data. The principle idea of the denoising process is keeping those coefficients which are necessary to reconstruct the signal unchanged and setting others to zero. In our case, according to results of modeling, only the first eight detail coefficients are needed. The method has been validated on both synthetic and field BHTEM raw data. Besides the DWT, complementary measures are introduced accordingly. For simple data set, a curve fitting technique is employed to smooth the signal furthermore. For field BHTEM raw data the correlation analysis is carried out to identify and correct distorted transients. The efficiency and reliability of the method are proven by the results.

Keywords: discrete wavelet transform; denoising; borehole TEM.

1. Introduction

The transient electromagnetic (TEM) methods are an indispensable tool in geophysical exploration, especially for metallic ore deposits discovery. A TEM survey can be conducted on different platforms: on the earth's surface (ground TEM), on an airplane (ATEM), and down to a borehole (BHTEM). The BHTEM, after more than three decades of development, has become a routinely used approach in searching for concealed deposits around boreholes and deep located economic targets. In contrast to conventional borehole logging, which studies in detail the properties of rocks intersected by the borehole, BHTEM investigates a large volume of earth around the borehole. Therefore, it increases significantly the effective detection radius. In a BHTEM survey, one or multiple large transmitter loops are laid out on the surface and a receiver moves downhole (Lamontagne and Milkereit, 2007). A typical configuration of BHTEM is illustrated in Figure 1.

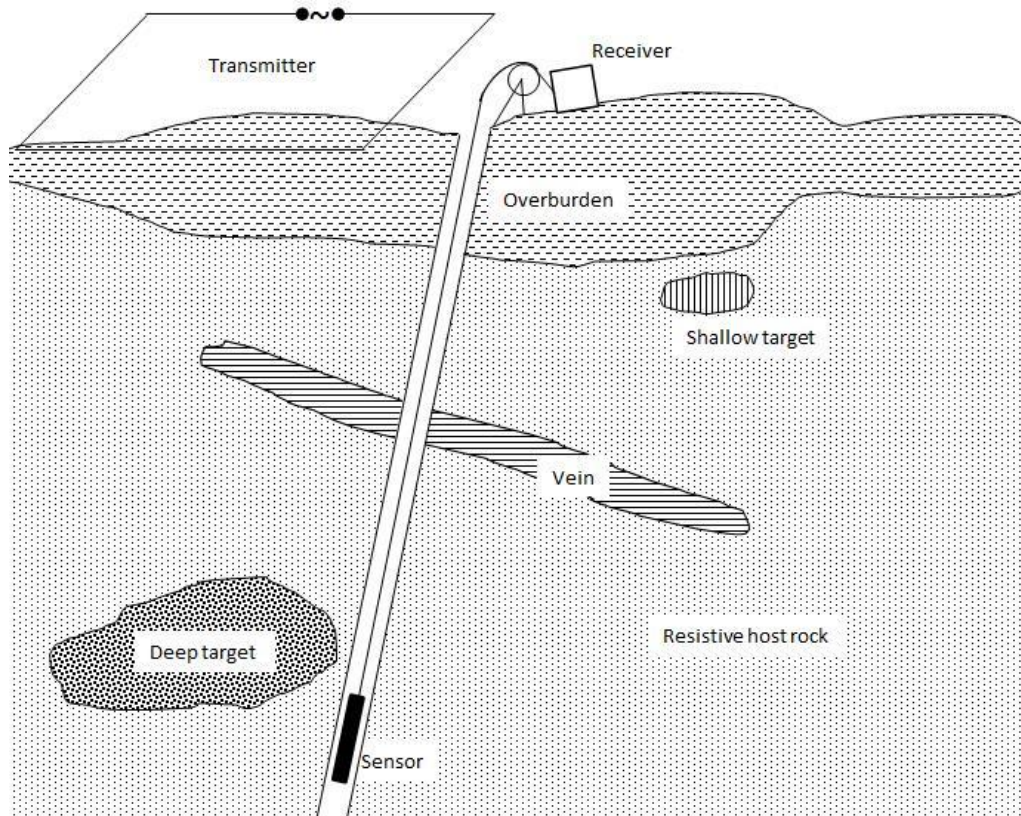


Figure 1: Geoelectric cross section illustrating the application of the BHTEM in exploring deep targets (adapted from Dyck, 1981).

In processing TEM data, noise is always a major problem to cause misinterpretation. While denoising is essential, an almighty denoising method does not exist, because data collected by different TEM methods suffer from different kinds of noise. For airborne TEM surveys, the data are often contaminated by the motion-induced noise (due to the movement of the receiving coil and wind) and sferics. Wang et al. (2013) proposed a wavelet-based method to correct the movement-induced baseline drift. In addition, Nenna and Pidlisecky (2013) used the continuous wavelet transform (CWT) to identify culture noise and topographic features in an ATEM groundwater survey. Bouchedda et al. (2010) also used the wavelet transform in ATEM data enhancement by reducing the sferics. For ground TEM, the effect of cultural noise, such as noise induced by the nearby building and power lines becomes more apparent. Ji et al. (2016) combine the wavelet threshold

method and stationary wavelet transform to remove background noise and random spikes from TEM data.

In BHTEM, the situation is different from that of ATEM and ground TEM. On one hand, because of the screen effect of the earth, the intensity of spherics and cultural noise is reduced in the borehole. On the other hand, the sensor may rotate, the pathway of a borehole may be not smooth, fluid may exist, and underground infrastructures interfere with the primary EM field in deep mine area; they all could be sources of noise for BHTEM measurement. These features of BHTEM lead to a need for an efficient denoising method. We present a new strategy of denoising for BHTEM raw data in this paper. The proposed method is mainly based on discrete wavelet transform (DWT), and two complementary methods are involved according to features of the data set. The curve fitting method is used when the measurement is not repeated, like in theoretical studies. For repeated measurements, like in most field surveys, we use the correlation analysis to remove residual noises.

2. Methods

2.1 Discrete wavelet transform (DWT)

Similar to the Fourier transform (FT), which transforms a time domain signal into a sum of triangular functions, the wavelet transform (WT) decomposes a signal into different scale components. In comparison with the FT, the WT retains the time information of an event, which is lost in the FT. This is a key advantage of the WT in analyzing non-stationary signals. The theory of the WT and its numerical implementation have been documented in detail in many literatures (Daubechies, 1992; Kumar, 1997). A brief introduction is given below.

The one-dimensional continuous wavelet transform (CWT) of a signal $f(t)$ is given by

$$w(s, \tau) = \int_{-\infty}^{\infty} f(t) \Psi_{s,\tau}^*(t) dt, \quad (1)$$

where s and τ are the scale parameter and the translation along the time axis, respectively, and the $*$ is the complex conjugate operator. $\Psi_{s,\tau}^*(t)$ is the scaled and translated version of the mother wavelet ψ

$$\Psi_{s,\tau}^*(t) = \frac{1}{\sqrt{s}} \psi^*\left(\frac{t-\tau}{s}\right). \quad (2)$$

Through equations (1) and (2) we can see that in the one-dimensional CWT the signal is analyzed by functions generated by scaling and translating the mother wavelet. In discrete wavelet transform (DWT), a scaling function (ϕ) is introduced

$$\phi_{j,k}(t) = 2^{j/2} \phi(2^j t - k).$$

And the DWT of the signal $f(t)$ is written as

$$f(t) = \sum_{k=-\infty}^{\infty} A_N(k) \cdot \phi_{j,k}(t) + \sum_{j=1}^N \sum_{k=-\infty}^{\infty} D_j(k) \Psi_{j,k}(t), \quad (3)$$

where A_N is the approximation coefficients at level N , and D_j is the detail coefficients at level j . A_N can be obtained through inner product of the signal and the scaling function; and D_j is computed via inner product of the signal and the wavelet function

$$A_N(k) = \int_{-\infty}^{\infty} f(t) \cdot \phi_{N,k}(t),$$

$$D_j(k) = \int_{-\infty}^{\infty} f(t) \cdot \Psi_{j,k}(t).$$

The application of denoising with the DWT is generally implemented by comparing the detail coefficients with a threshold value: if the absolute value of the coefficient is not smaller than the threshold, it is kept unchanged; otherwise, it will be changed accordingly: set to zero (hard thresholding) or shrink towards zero (soft thresholding). However, in our

method the strategy of processing the detail coefficients to eliminate noise is determined according to the characteristic of the BHTM signal, which decays rapidly just after the power-off, and then slowly diminishes to zero. By combining this transient characteristic and the fact that detail coefficients in DWT represent the transient events, it is reasonable to hypothesize that there will be only a few non-zero detail coefficients corresponding to the duration of the fast decay process in each decomposition level. Therefore, our strategy is: detail coefficients corresponding to the fast decay process are kept unchanged, and others are set to zero. The key question is which and how many detail coefficients are needed to reconstruct the signal.

To find out the answer, a series of numerical modeling has been implemented. During the process of modeling we found that only the first several detail coefficients from each level are not zero. To reconstruct the signal, only these non-zero coefficients are needed. However, coefficients needed from different levels are different. For example, with a decomposition level of 10 the first several detail coefficients needed from each level to properly reconstruct the signal are: 6,7,7,8,8,8,8,8,8,8 (level 1 to level 10). But they may be influenced by the decomposition level. Based on our modeling the signal can be perfectly reconstructed with the first eight coefficients of each level for all decomposition levels. Hence, in the process of denoising of our method we keep the first eight coefficients of each level and set all others to zero. Figure 2 shows that the signal reconstructed with the first eight detail coefficients perfectly coincides with the original signal; however, if coefficients kept are less than eight, the reconstructed signal will be distorted, which is resulted from insufficient information.

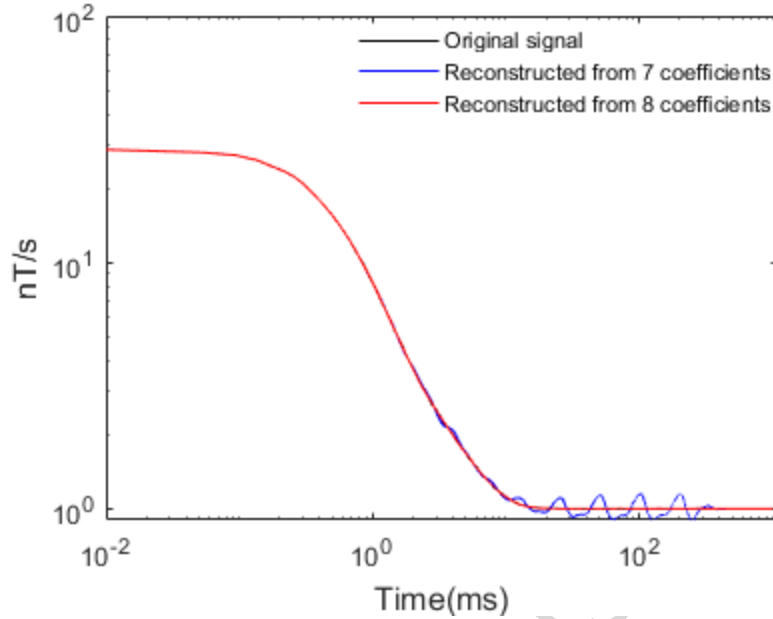


Figure 2: Comparison of the original signal and the reconstructed signal

The performance of wavelet denoising largely depends on two factors: selection of the mother wavelet and the number of decomposition levels. The symlets family is chosen for their orthogonality and near symmetry properties. To find out which specific wavelet in the symlets family is the most suitable one, an iterative comparison of trial and error is implemented. The noisy signal used in this process is synthesized by adding noises (Figure 5) to the signal (Figure 4). According to the results, ‘sym5’ is selected. In addition, a low decomposition level can lead to inferior denoising results; while, a too high decomposition level may introduce distortions. Different decomposition levels are attempted by using ‘sym5’, it is the tenth decomposition level gives us the best result (Table 2). The signal-to-noise ratio (SNR), which is calculated by Equation (4), of trying different wavelets and decomposition levels are listed in Table 1 and Table 2, respectively.

$$\text{SNR} = 10 \times \log_{10} \frac{P_{\text{signal}}}{P_{\text{noise}}}, \quad (4)$$

where P_{signal} and P_{noise} are the power of the signal and the power of the noise, respectively. Given a signal $s(n)$, ($n = 1, 2, 3, \dots, N$, N is the total amount of samplings.) the power of this signal is $P = \frac{1}{N} \sum_{n=1}^N s(n)^2$.

Table 1: Applying different wavelets on a noisy signal with an SNR of 15dB.

Wavelet	'sym1'	'sym2'	'sym3'	'sym4'	'sym5'	'sym6'	'sym7'
SNR(dB)	33.39	33.47	34.27	35.71	35.72	29.00	19.23

Table 2: Trying different decomposition levels on a noisy signal with an SNR of 15dB.

Decomposition level	6	7	8	9	10	11	12
SNR(dB)	26.89	27.97	32.79	35.17	35.72	35.71	35.39

The DWT based method stated above can reject most part of the noise; however, it has an inherent weakness. The first eight coefficients, which are kept unchanged, can also be contaminated by noise. The reason of letting these eight coefficients unprocessed is that it is difficult to obtain a proper estimation of the threshold for them. These residual noises may influence the decay process of the signal and thus affect the estimation of the time constant of the target. Therefore, complementary measures are needed to suppress the influence of the residuals.

2.2 Curve fitting technique (CFT)

When the signal is a simple data set, which means the measurement is not repeated many times. This refers to theoretical studies or field measurements with limited time and/or budgets. In this case, the curve fitting technique (CFT) is used as a complementary measure to improve the denoising result.

In consideration of the transient characteristics of the BHTEM data, the following exponential equation is considered as the fitting model (Nabighian and Macnae, 1991):

$$s(t) = \alpha \cdot e^{-t/\tau}, \quad (5)$$

where α and τ are parameters to be determined, they denote the gain parameter and the time constant of the conductor, respectively.

The fitting function is calculated via the least square criterion. The CFT is used for post-processing of BHTEM in an effort to reduce the influence of the residual perturbation after DWT process. To constrain the fitting result, fractions of perturbation in the signal are identified and excluded from the fitting process.

2.3 Correlation analysis

Generally, in a BHTEM field survey, the measurement is repeated many times at each survey point. Each measurement is called a transient. In the end, all transients are stacked into one record to reduce random noise. Since repeated measurements at a certain survey point are basically recording signals from the same source, without distortion there should be a strong linear correlation between all transients. However, as we mentioned previously, during the measurement of BHTEM the sensor may rotate and/or vibrate because of the liquid flow or obstacles in the borehole. This rotation and/or vibration will distort certain transients during the measurement. So if certain transients have bad correlations with other transients, they are considered as distorted transients.

To find out the distorted transients, we use correlation analysis. The Pearson correlation coefficient is chosen because of its invariance, i.e., the coefficient is not affected by separate changes in the two variables in location and scale. For example, if one variable X is changed to $\alpha X + \beta$, and the another variable Y is changed to $\lambda Y + \gamma$, where α , β , λ ,

and γ are constants, and $\alpha, \lambda > 0$, the correlation coefficient will not be changed. The coefficient between two variables X and Y is calculated by the formula:

$$\rho_{X,Y} = \frac{\text{cov}(X,Y)}{\sigma_X\sigma_Y}, \quad (6)$$

where, $\text{cov}(X,Y)$ calculates the covariance between variables X and Y; σ_X and σ_Y are the standard deviation of X and Y, respectively.

The correlation coefficient calculated by equation (6) ranges from -1 to 1. The value of 1 means there is a perfect linear relationship between the two variables. The value of -1 implies that the two variables still have a linear relationship, but they change in the opposite direction. When the correlation coefficient equals to zero, there is no linear correlation between the two variables.

After the distorted transient is identified with the help of correlation analysis, it is replaced by linear interpolation using other transients. The interpolation is carried out sampling by sampling, i.e., we first take the first sampling of undistorted transients to do linear interpolation to replace the first sampling of the distorted transient. Then we repeat this process on other samplings until the entire distorted transient is replaced.

3. Method validation

To verify the reliability of the method, it has been tested on both synthetic and field BHTEM data.

3.1 Application on synthetic data

The synthetic BHTEM data (Figure 4) are generated using Loki, which is a 3D forward modeling program (Raiche *et al.*, 2007). The model (Figure 3) used to generate the data contains a prismatic conductor (5 ohm·m) in a homogeneous half-space (3000 ohm·m).

Three types of noise (Figure 5) are added to the synthetic data. Except for the spherics,

which is from field measurements, the other two types of noise are generated by Matlab.

The SNR, computed by equation (4), of the noisy signal (Figure 6) is 15dB.

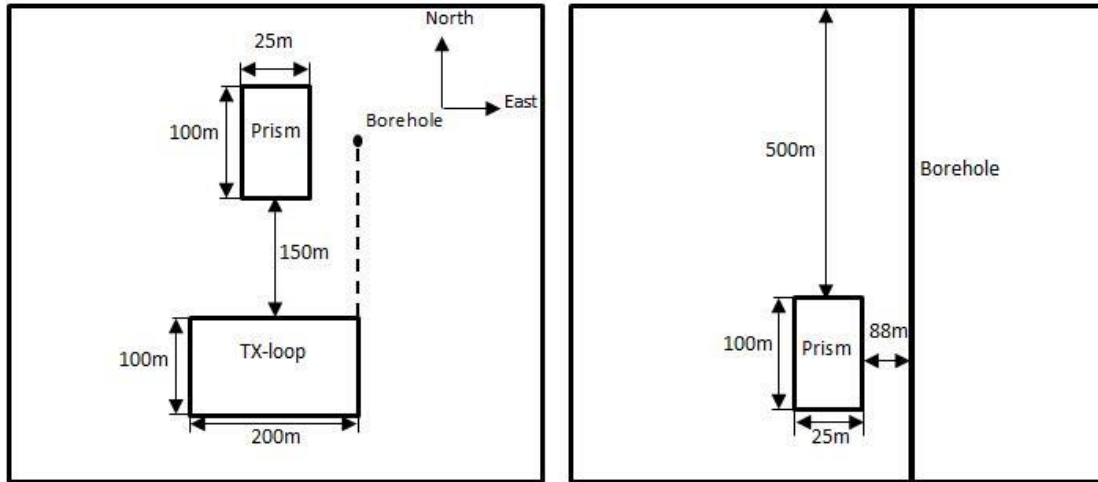


Figure 3: The model used to generate synthetic data. (a) Top view of the model. (b) Cross-section view of the model.

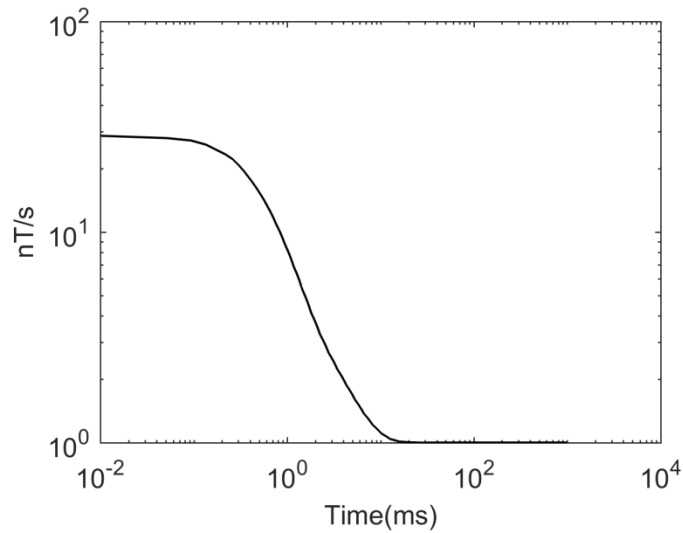


Figure 4: A BHTEM signal generated by Loki with the model shown in Figure 3.

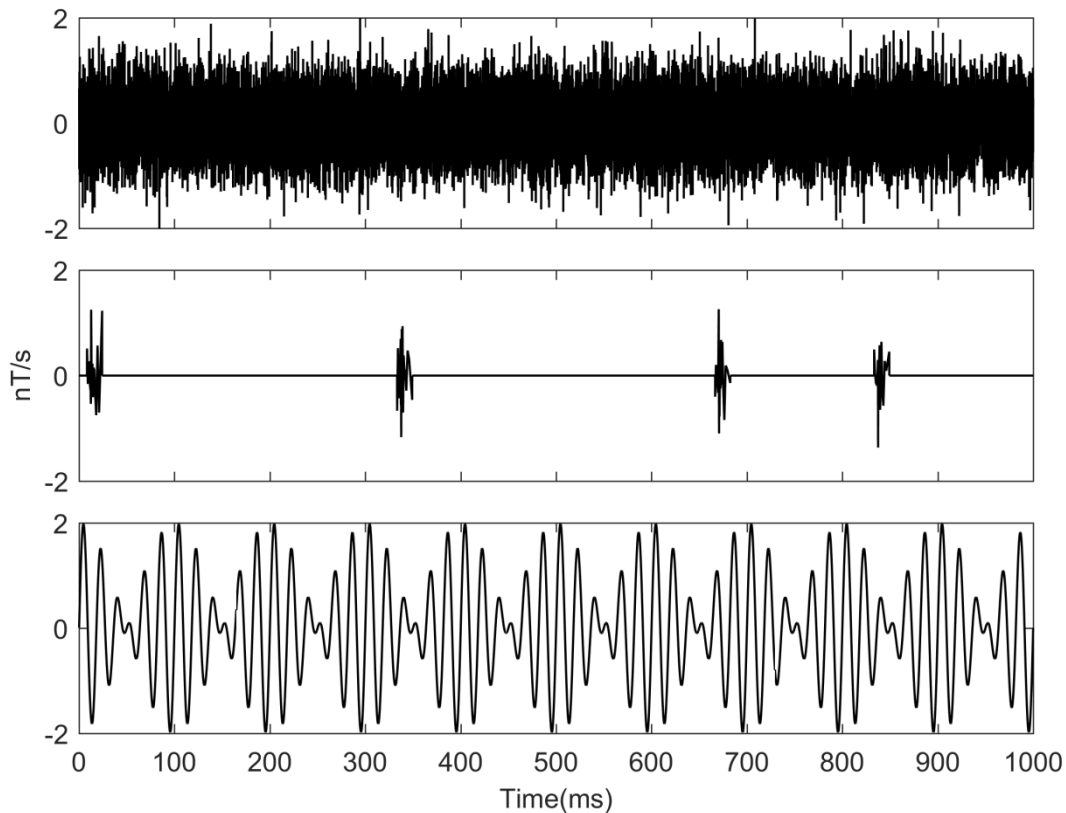


Figure 5: Three types of noise added to synthetic data. From top to bottom: random noise, sferics, and noise from the power line (50 and 60 Hz).

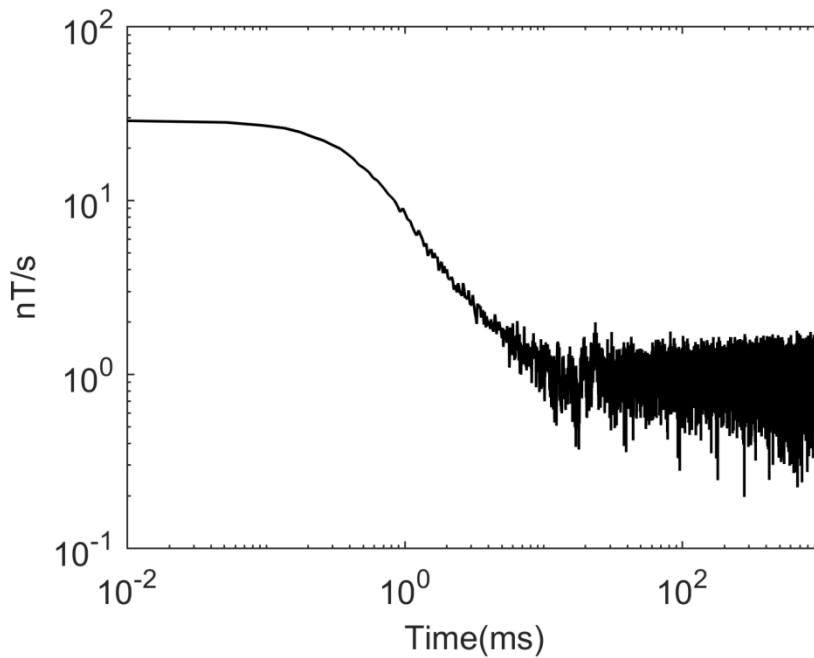


Figure 6: Generated noisy signal with an SNR of 15dB.

To test our method, the noisy signal is first processed with the DWT. Figure 7 presents the result. After this process, most part of the noise has been removed; the SNR is significantly improved from 15dB to 35dB. However, a small portion of noise remained. The signal is further processed by CFT, and the comparison is shown in Figure 8.

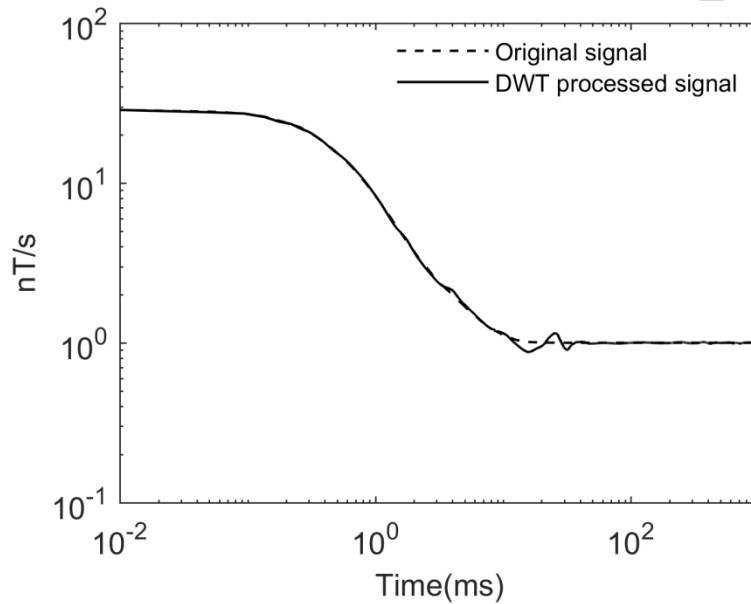


Figure 7: Denoising result when only using DWT.

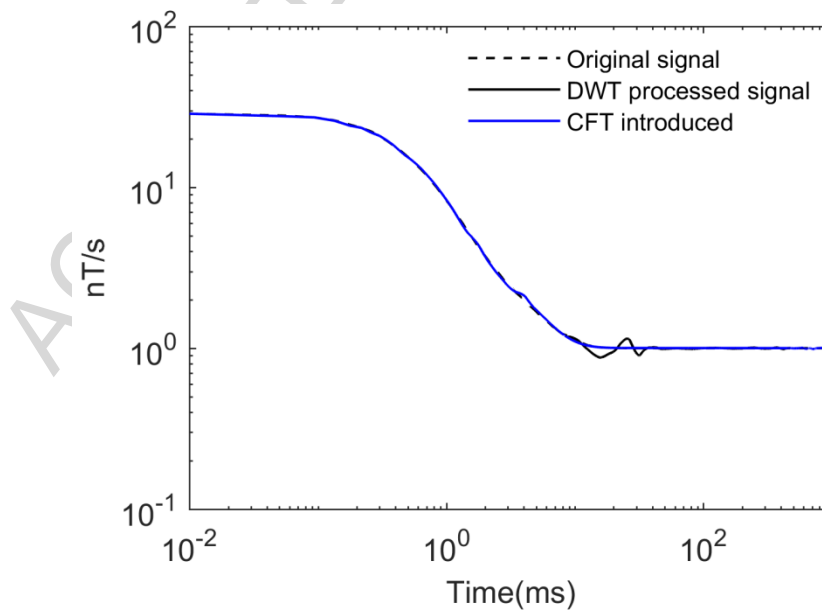


Figure 8: Comparison of denoising results.

To give a quantitative evaluation of the effectiveness of the method, apart from the SNR two more statistic parameters are calculated. They are the relative error, Equation (7), and the mean squared error (MSE), Equation (8).

$$\delta x_n = \left| \frac{x_n - x'_n}{x_n} \right|, n = 1, 2, 3, \dots, N; \quad (7)$$

$$\text{MSE}(x) = \frac{1}{N} \sum_{n=1}^N (x_n - x'_n)^2; \quad (8)$$

where x and x' represent the original noise-free signal and the denoised signal, respectively. N is the total number of the samplings. The relative error curves are shown in Figure 9, and the MSE and SNR are listed in Table 3.

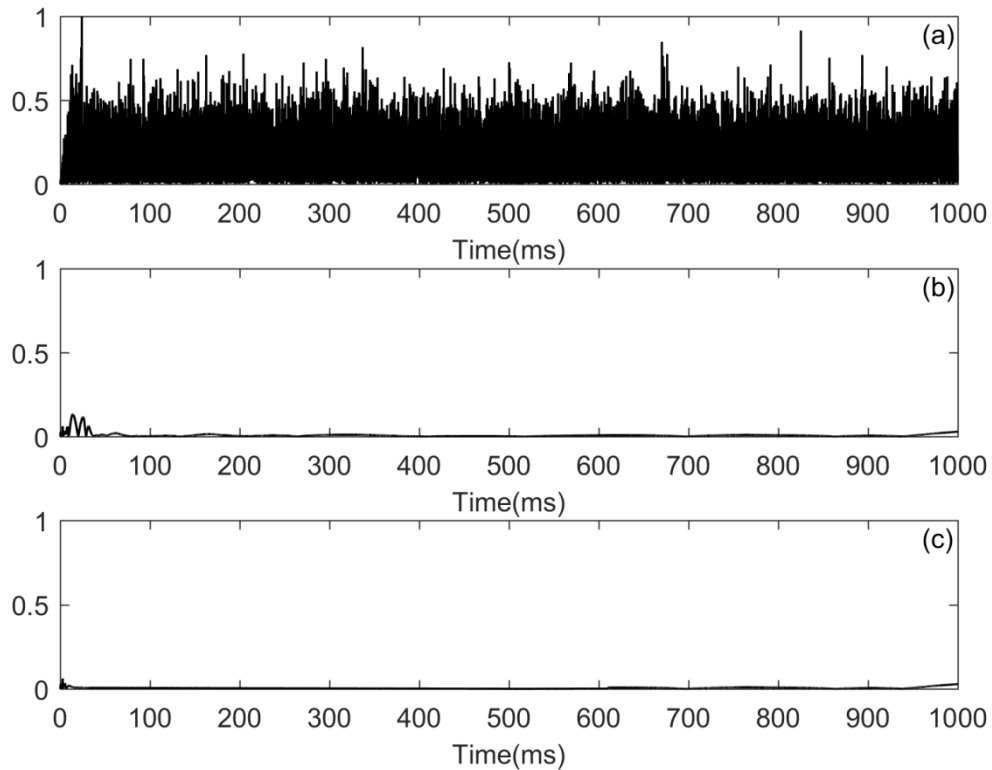


Figure 9: Relative error curves, (a) the error curve of the noisy signal, (b) the error curve of the denoised signal when only DWT is used, (c) the error curve of the denoised signal after DWT and CFT.

Table 3: A comparison of MSE and SNR.

Signal	MSE	SNR(dB)
Noisy signal	0.044	15.0
Signal processed by DWT	3.702×10^{-4}	35.7
Signal processed by DWT and CFT	0.907×10^{-4}	41.8

According to the relative error curves and the MSE and SNR values, the DWT method can effectively remove the most part of the noise; the CFT further improves the signal-to-noise ratio by removing local residual noise.

3.2 Application on field data

Abitibi Geophysics Inc. provided the field data used in this study. The sensor used in the measurement is the DigiAtlantis, which is a product of ElectroMagnetic Imaging Technology (EMIT). It can acquire simultaneously three components (coaxial component A ; component U which is perpendicular to A , and component V which is perpendicular to the $A-U$ plane). The sampling frequency of the measurement is 24 kHz, and the base frequency is 0.25 Hz; the duty cycle is 0.5. The recorded raw data is in mV (not converted to nT), which is different from the synthetic data as shown before.

Based on the synthetic model, 8 detail coefficients were kept unchanged during the process of denoising with the DWT. We do first verify with field data if 8 detail coefficients are still the right number. Figure 10 shows the results that use less or more than 8 detail coefficients to process the noisy data (randomly choosing one measurement of V -component). The conclusion is unchanged.

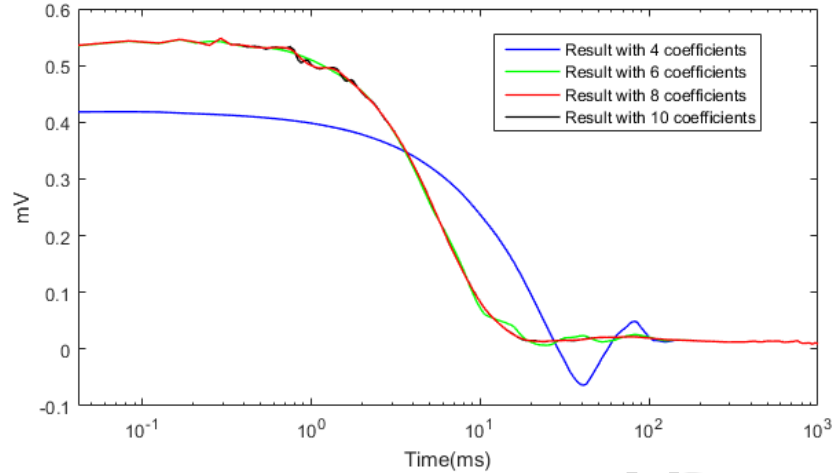


Figure 10: An example comparing results obtained with different numbers of detail coefficients.

BHTEM field data are much more complicated than synthetic data. The measurement at each survey station is repeated for up to hundreds of times to improve data quality. But during the period of measurement, other sorts of noise, in addition to the three types considered in the synthetic data processing, may come from the electronic instability and the movement of the sensor. Certain measurements will be distorted by these noises. Fortunately, the repeated measurement mechanism provides us with a way to identify the distorted measurements and then correct them accordingly. The strategy of processing BHTEM field data will be slightly different from that of processing the synthetic data. Detailed steps of processing real BHTEM field data are as follows.

1. Denoise raw data using the DWT. Since every transient could be affected differently by the noise, every transient is denoised individually using the DWT. After processed via DWT some transients could be still distorted. The biggest advantage of denoising raw data instead of stacked data is that those distorted transients can be identified and corrected afterward. This can reduce distortion and preserve useful information.

2. Identify distorted transients through correlation analysis. We take a certain percentage of the measurement, which has the worst linear correlation with other transients, as distorted transients; and replace these distorted transients via linear interpolation.
3. Stacking processed raw data. Stacking is a fundamental and rudimentary process to reduce noise in TEM data processing. It is a process of averaging a series of transients. As it is a process of averaging, it has a limited effect on reducing non-random noise. Examples are presented later to demonstrate the advantage of using denoised raw data to stack. In this study, Halverson stacking is chosen for its ability to remove linear drift (Kingman *et al.*, 2004).

Since the three components (A , U , and V) may be affected differently by noise, three examples are presented separately below, one example for each component. Please keep in mind that these examples are chosen to represent different scenarios, they are not necessarily from the same survey point.

Component-A: There are 128 transients in the recording (Figure 11). From the figure, the signal can be divided into two segments based on the drift situation. The first segment, which has no drift, consists of the first 34 transients. The second segment, which drifts linearly, is composed of the last 94 transients. Each segment is processed separately.

The noise level in this data set is very low. There is no obvious difference between the original raw data (Figure 11(a)) and those denoised by the DWT (Figure 11(b)). Nevertheless, the abrupt change of the drift situation causes the distortion of the 34th transient, as red arrows indicate in Figure 11(a). The distortion is not corrected (Figure 11(b)) until the correlation analysis is implemented (Figure 11(c)).

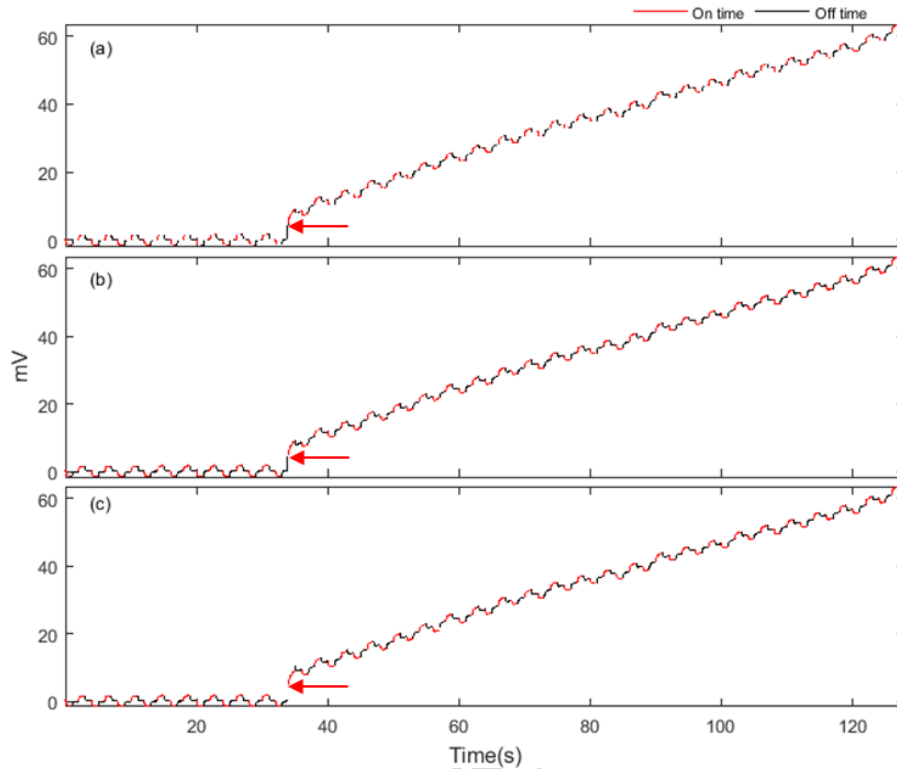


Figure 11: Raw data of component-A. (a) Original raw data, (b) denoised raw data, (c) denoised raw data with distortion corrected.

Stacked signals for on-time transients and off-time transients are presented in Figure 12. No apparent difference is spotted between stacked on-time signals when we use different raw data sets, because the noise level is very low in this data set, and the only distorted transient occurs in off-time transients. However, for stacked off-time signals, after the distorted transient is corrected the stacked result is improved a lot. This example shows that one single distorted transient will significantly affect the stacked result. It proves the necessity to identify and correct the distorted transients.

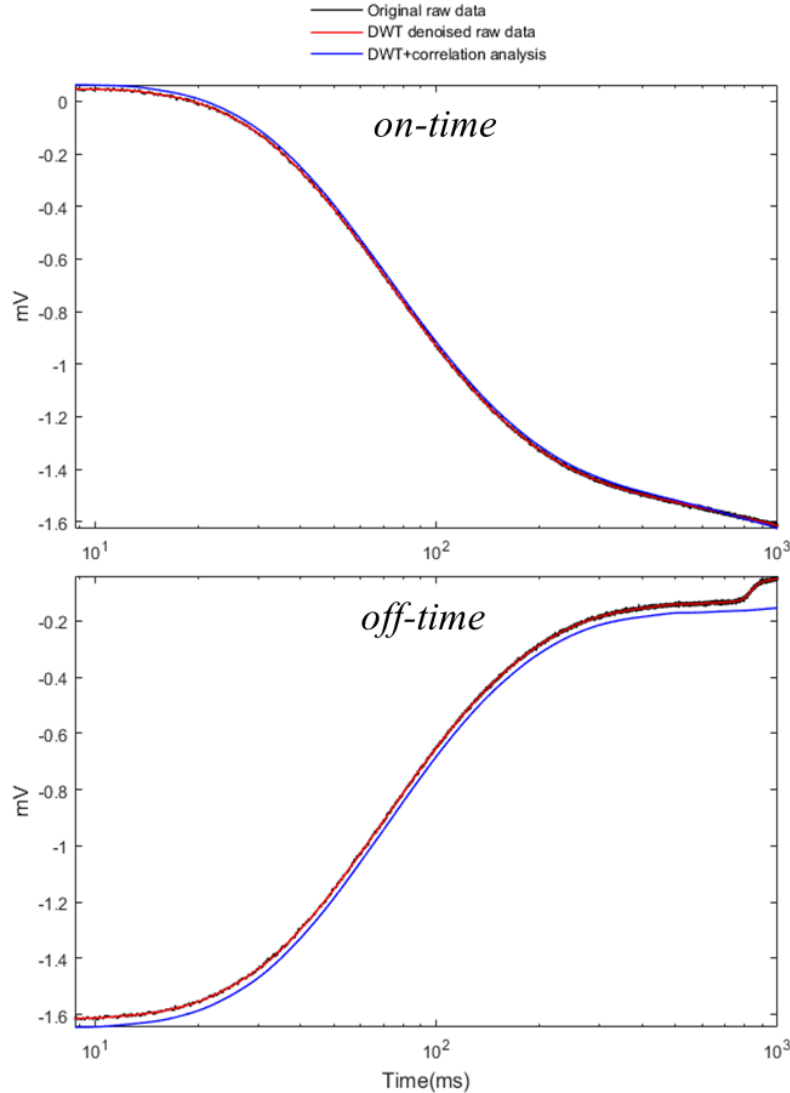


Figure 12: The stacked signals obtained by using different raw data sets of component-A.

Component-U: There are also 128 transients in this data set (Figure 13). The segmentation of this data set is much more complicated than the previous example. Since after distorted transients are identified, they will be replaced through linear interpolation of other transients, we should keep the drift as linear as possible in each segment. The data set is divided into five segments: (1) transients 1 to 12; (2) transients 13 to 44; (3) transients 45 to 60; (4) transients 61 to 118; and (5) transients 119 to 128. Compared with the previous example, the noise level in this data set is higher, and the distortion is more

severe. After denoised by the DWT most noise is eliminated (compare Figure 13(a) and (b)), whereas, distortions remain unchanged (Figure 13(b)). After the distorted transients in the data set are identified by correlation analysis, they have been corrected accordingly (Figure 13(c)).

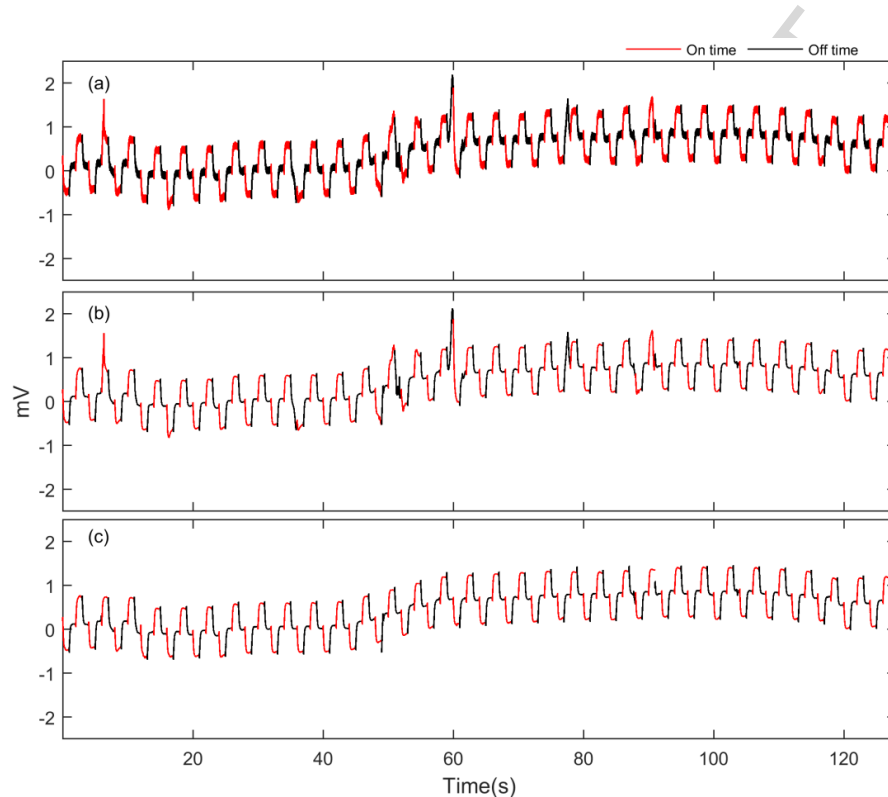


Figure 13: Raw data of component- U . (a) Original raw data, (b) denoised raw data, (c) denoised raw data with distortion corrected.

Figure 14 presents stacked signals for on-time transients and off-time transients. Applying the DWT on the data set certainly improves the quality; however, there is no apparent difference in the shape of the curve between signals stacked from original raw data and the DWT denoised raw data. After distortions are remedied, stacked curves become smoother and more reasonable.

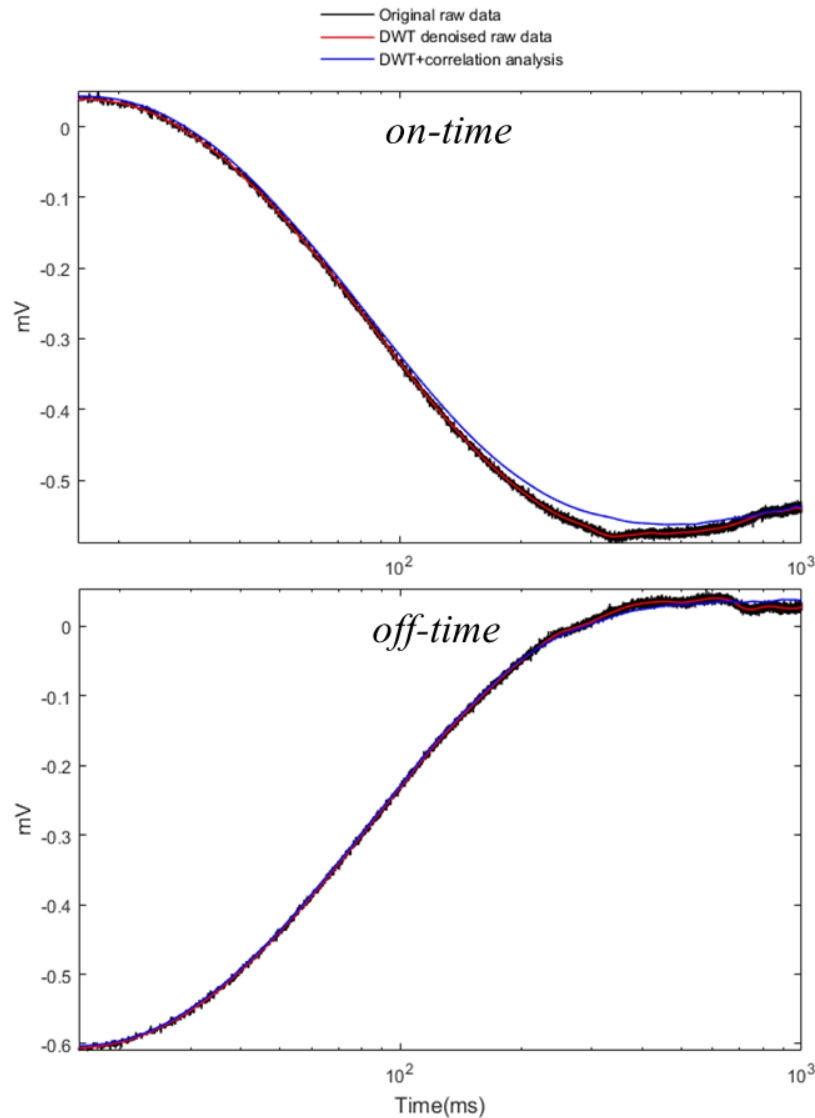


Figure 14: The stacked signals obtained by using different raw data sets of component-U.

Component-V: Same as data sets in the two previous examples, there are 128 transients in this recording (Figure 15). No obvious change in drift situation is observed, so the data set will be treated together, i.e., no segmentation is needed.

The most obvious feature of this data set is that the noise level is moderately high, the amount of distorted transients is large, and the distortion is severe. Similarly, after the application of DWT noise level is lowered a lot (compare Figure 15(a) and (b));

distortions remain unchanged (Figure 15(b)). Only after the use of correlation analysis distorted transients in the data set are corrected effectively (Figure 15(c)).

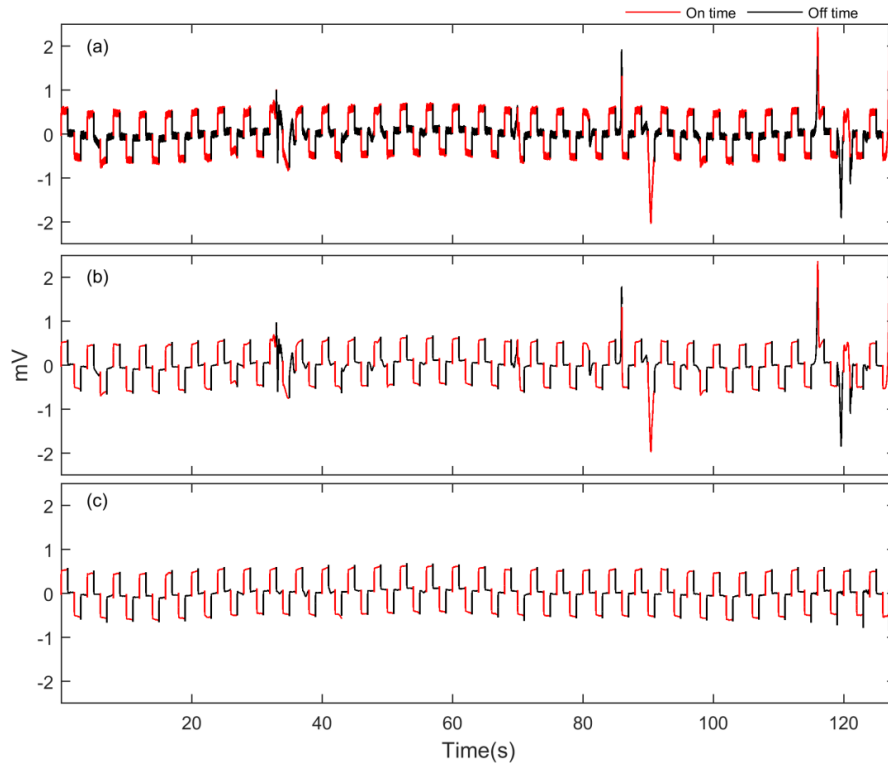


Figure 15: Raw data of component-V. (a) Original raw data, (b) denoised raw data, (c) denoised raw data with distortion corrected.

As presented in the two previous examples, the denoising process with the DWT does improve the quality of the signal, whereas it is not able to reduce the influence of distorted transients on the result of stacking (Figure 16). The correlation analysis is indispensable to identify distorted transients in a data set.

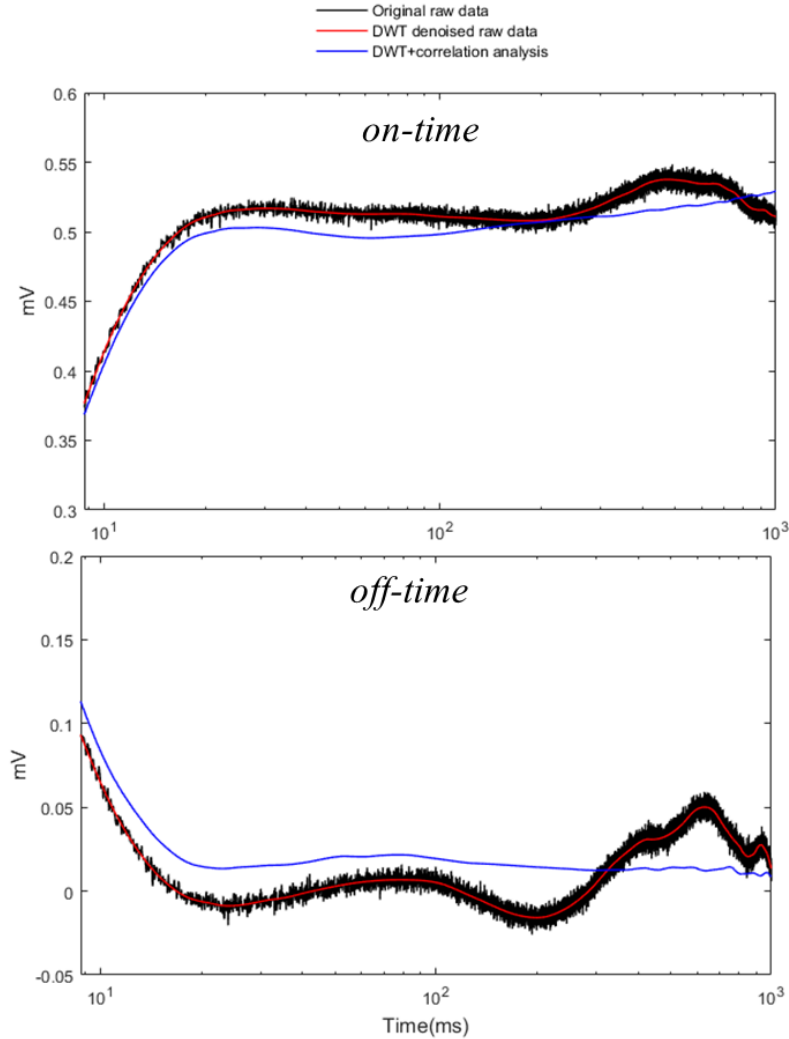


Figure 16: The stacked signals obtained by using different raw data sets of component-V.

4. Conclusion

The presented wavelet-based technique combines the wavelet's ability to detect transient events and the unique characteristics of the BHEM signal. The application of our method is not limited by the nature of the noise; also there is no need to locate the noise in the signal.

Applications on synthetic and survey data show that using the DWT alone can considerably reduce the noise level, but the noise residual may still have negative influences on future interpretations. Different complementary measures are taken to

reduce local residual noises. For simple data sets, the residual is caused mainly by the noise retained in the unprocessed detail coefficients. In this case, we use the curve fitting method to smooth the signal. For survey data with repeated measurements, the residual is mainly because of distorted transients in the raw data. Those distortions can be caused by the instability of the equipment and the oscillation of the sensor. To reduce its influence, the correlation analysis is implemented.

One thing to be noticed is that the decomposition level and the wavelet in our method are chosen based on characteristics of our data; adjustments are expected for different data sets.

5. Acknowledgment

This work is funded by FRQNT (le Fonds de Recherche du Québec - Nature et Technologies) with industry partners Abitibi Geophysics Inc. and LaRonde Mine of Agnico Eagle Mines Limited. Abitibi Geophysics Inc. is particularly thanked for providing access to geophysical data as well as valuable discussions with us through the project.

References

1. Augustin, A.M., Kennedy, W.D., Morrison, H.F. and Lee, K.H., 1989. A theoretical study of surface-to-borehole electromagnetic logging in cased holes. *Geophysics*, 54(1), pp.90-99.
2. Bouchedda, A., Chouteau, M., Keating, P. and Smith, R., 2010. Sferics noise reduction in time-domain electromagnetic systems: application to MegaTEMII signal enhancement. *Exploration Geophysics*, 41(4), pp.225-239.
3. Daubechies, I., 1992. Ten lectures on wavelets (Vol. 61). Siam.
4. Dyck, A.V., 1981, A method for quantitative interpretation of wideband, drill-hole EM surveys in mineral exploration: Doctoral dissertation, University of Toronto.
5. Ji, Y., Li, D., Yu, M., Wang, Y., Wu, Q. and Lin, J., 2016. A de-noising algorithm based on wavelet threshold-exponential adaptive window width-fitting for ground electrical source airborne transient electromagnetic signal. *Journal of Applied Geophysics*, 128, pp.1-7.
6. Ji, Y., Li, D., Yuan, G., Lin, J., Du, S., Xie, L. and Wang, Y., 2016. Noise reduction of time domain electromagnetic data: Application of a combined wavelet denoising method. *Radio Science*, 51(6), pp.680-689.
7. Killeen, P.G. ed., 1986. Borehole geophysics for mining and geotechnical applications. Canadian Government Publishing Centre and Services Canada.
8. Kingman, J.E., Halverson, M. and Garner, S.J., 2004. Stacking of Controlled Source Electrical Geophysical Data.
9. Kumar, P. and Foughoula - Georgiou, E., 1997. Wavelet analysis for geophysical applications. *Reviews of geophysics*, 35(4), pp.385-412.

10. Lamontagne, Y. and Milkereit, B., 2007. Deep exploration with EM in boreholes. Exploration in the new millennium, pp.401-415.
11. Lei, L., Wang, C. and Liu, X., 2013. Discrete wavelet transform decomposition level determination exploiting sparseness measurement. International Journal of Electrical, Computer, Energetic, Electronic and Communication Engineering, 7(9), pp.691-694.
12. Macnae, J.C., Lamontagne, Y. and West, G.F., 1984. Noise processing techniques for time-domain EM systems. Geophysics, 49(7), pp.934-948.
13. Michael, W., 2007. Digital signal processing using MATLAB and wavelets. Infinity.
14. Misiti, M., Misiti, Y., Oppenheim, G. and Michel, J.P., 1996. Wavelet toolbox: for use with MATLAB.
15. Nabighian, M.N. and Macnae, J.C., 1991. Time domain electromagnetic prospecting methods. Electromagnetic methods in applied geophysics, 2(part A), pp.427-509.
16. Nenna, V. and Pidlisecky, A., 2013. The use of wavelet transforms for improved interpretation of airborne transient electromagnetic data. Geophysics, 78(3), pp.E117-E123.
17. Percival, D.B. and Walden, A.T., 2006. Wavelet methods for time series analysis (Vol. 4). Cambridge university press.
18. Polzer, B., 2000. The role of borehole EM in the discovery and definition of the Kelly Lake Ni-Cu deposit, Sudbury, Canada. In SEG Technical Program Expanded Abstracts 2000 (pp. 1063-1066). Society of Exploration Geophysicists.
19. Raiche, A., Sugeng, F. and Wilson, G., 2007. Practical 3D EM inversion? The P223F software suite. ASEG Extended Abstracts, 2007(1), pp.1-5.

20. Ridsdill-Smith, T.A. and Dentith, M.C., 1999. The wavelet transform in aeromagnetic processing. *Geophysics*, 64(4), pp.1003-1013.
21. Wang, Y., Ji, Y., Li, S., Lin, J., Zhou, F. and Yang, G., 2013. A wavelet-based baseline drift correction method for grounded electrical source airborne transient electromagnetic signals. *Exploration Geophysics*, 44(4), pp.229-237.

ACCEPTED MANUSCRIPT

Highlights :

- Applied on TEM raw data to eliminate noise and distortions.
- Complementary methods are introduced according to signal's feature.

ACCEPTED MANUSCRIPT